QUANTIFYING LAND COVER CHANGE IN ZADAR (2017–2025) USING PLANET SCOPE IMAGERY

DOI:
UDC: [502.52:711.4]-043.7:528.85.044.8(497.5)"2017/2025"

Rina Milošević
Center for Geospatial Technologies, University of Zadar
Department of Ecology, Agronomy and Aquaculture, University of Zadar

ABSTRACT

This study quantifies land cover change in the City of Zadar between 2017 and 2025 using PlanetScope imagery and Machine Learning classification. Spectral bands were complemented with spectral indices (NDVI, VARI, Brightness, BSI) and a NIR-based texture measure to improve class separability. Random Forest and XGBoost algorithms were evaluated using stratified five-fold cross-validation, while a transfer experiment was conducted to assess temporal robustness. Epoch-specific models achieved high classification accuracy (ACC ≈ 0.94–0.95; ROC AUC ≈ 0.96–0.98), whereas direct model transfer from 2017 to 2025 resulted in reduced performance (ACC = 0.75), confirming the presence of temporal domain shift. At the city scale, impervious surfaces expanded proportionally from 27% to 29%, accompanied by a slight decline and fragmentation of urban green spaces. Hexagon-based spatial analysis identified spatially coherent zones of impervious surface growth, indicating structurally organized urban expansion. The results suggest continued conversion of green areas. Future research should explore multi-annual or sub-annual satellite time series and advanced domain adaptation approaches to improve model generalization across temporal domains.

Keywords: Urban land cover, PlanetScope, Machine learning, Temporal domain shift, GIS analysis

INTRODUCTION

Urbanization represents one of the most pronounced forms of contemporary land cover transformation. Since 2007, more than half of the global population has resided in cities, and this proportion is expected to continue growing [1]. The expansion of built-up areas replaces natural and semi-natural surfaces with impervious materials, altering hydrological processes, increasing runoff, and contributing to ecological fragmentation. Mediterranean cities are particularly vulnerable to these pressures due to their long-term urban continuity and increasing susceptibility to climate extremes [2]. Urban green spaces play a critical role in climate regulation, flood mitigation, biodiversity support, and human well-being [3], [4]. However, rapid urban growth frequently results in their reduction and fragmentation. Monitoring land cover dynamics is therefore essential, particularly in cities exposed to extreme rainfall and pluvial flood events. Understanding how urban expansion alters hydrological response is crucial for improving flood preparedness and supporting sustainable urban planning [5]. Advances in high-resolution satellite imagery and application of Machine Learning methods (ML) have significantly improved the ability to detect fine-scale urban change. PlanetScope imagery has already been applied in land use and land cover studies to quantify multi-temporal transformations in urban environments [6]. Its spatial resolution allows detailed discrimination of built-up surfaces, vegetation patches, and transitional land cover types, providing a suitable basis for systematic urban monitoring. Despite methodological progress, multi-epoch land cover analyses face the challenge of temporal domain shift, where models trained on one time period may not generalize reliably to another due to spectral variability and structural transformation [7]. This issue introduces uncertainty into change detection studies if not explicitly assessed. The City of Zadar represents an appropriate case study due to its documented expansion of impervious surfaces in recent years [8]. In addition, the extreme pluvial flood event of 11 September 2017 [9] highlighted the importance of understanding land cover structure in relation to urban vulnerability. This study aims to assess recent land cover transformation in Zadar between 2017 and 2025 using high-resolution satellite imagery and to evaluate the robustness of multi-temporal classification in the presence of temporal domain shift.

STUDY AREA

The study area covers the mainland part of the City of Zadar, located on the central Adriatic coast of Croatia, with an area of approximately 52 km² (Figure 2). Zadar is the administrative center of Zadar County and has undergone urban expansion over recent decades due to demographic and economic growth [10], [11], [12]. This development has resulted in increased impervious surface coverage and reduced urban green space [4]. Although Zadar exhibits long-term urban continuity and historically stable land cover distribution [2], the pace of transformation has intensified since the mid-twentieth century. Recent spatial analyses confirm the concentration of impervious surfaces in coastal urban zones, while vegetated areas remain dominant in the broader landscape [8]. The importance of monitoring land cover change was underscored by the extreme pluvial flood event of 11 September 2017, when 285 mm of rainfall fell within 24 hours, causing severe flash flooding [9]. Increasing exposure of Mediterranean cities to short-duration high-intensity rainfall has been widely reported [13]. In this context, quantifying changes in impervious and green surfaces is essential for understanding evolving urban vulnerability.

Figure 1. Study area - city of Zadar

MATERIALS AND METHODS

Satellite Data Acquisition and Preprocessing

The analysis is based on high-resolution PlanetScope satellite imagery with 3m spatial resolution for the City of Zadar acquired in June 2017 and June 2025 to ensure seasonal comparability. To maintain methodological consistency between epochs, only four common spectral bands (Blue, Green, Red, and NIR) were used. All rasters were atmospherically corrected and orthorectified prior to analysis. To minimize inter-annual radiometric differences, 2025 imagery was radiometrically normalized to the 2017 reference, and the normalized bands were used for index calculation and classification.

Derivation of Spectral and Texture Indices

To improve class separability, additional spectral indices and texture features were derived for both epochs. The Normalized Difference Vegetation Index (NDVI) was used to distinguish vegetated from non-vegetated surfaces, while the Visible Atmospherically Resistant Index (VARI) enhanced separation between vegetation, bare soil, and certain impervious materials. A Brightness index was calculated to represent overall surface reflectance, and the Bare Soil Index (BSI) was included to better identify exposed soil areas. In addition to spectral indices, a texture feature was computed as the local standard deviation of the NIR band (NIR_std) using a 5×5 moving window.

Classification samples collection

To minimize inter-epoch misclassification effects, reference samples were collected within stable land cover zones, defined as areas retaining the same class in both 2017 and 2025. Stable zones were identified through spatial intersection of class masks derived separately for each epoch. Vegetation was delineated using NDVI thresholds ($NDVI \geq 0.3$), while non-vegetated areas were separated using combinations of NDVI, VARI, and Brightness indices. Reference points were manually interpreted from 2017 orthophoto imagery provided by the Croatian State Geodetic Administration. Initial experiments using multiple detailed land cover classes resulted in substantial class confusion in 2025, likely due to radiometric variability and spectral overlap. To improve robustness and inter-annual consistency, classes were therefore aggregated into three broader categories: Urban Green Spaces (UGS) (wood, lawn), Impervious Surfaces (concrete, asphalt, stone), and Other (brown soil, macadam). This simplification reduced classification uncertainty while preserving the structural contrast between vegetated and built-up areas essential for change analysis.

Land cover model

Supervised classification was performed using two ensemble learning algorithms Random Forest (RF) and Extreme Gradient Boosting (XGBoost). Reference samples derived from stable land cover zones were used to train the models, with input features consisting of spectral bands, spectral indices, and texture measures. Model performance was evaluated separately for each epoch using stratified five-fold cross-validation to ensure balanced class representation across folds. Evaluation metrics included overall accuracy, macro-averaged ROC AUC (one-vs-rest), and macro-averaged Precision–Recall AUC, providing robust measures of both classification performance and class discrimination under potential class imbalance. To ensure methodological consistency for change detection, a reference model was trained on the full 2017 dataset and subsequently applied to classify both 2017 and 2025 imagery. RF was retained as the final mapping model due to its stable performance and comparable accuracy to XGBoost, while avoiding additional model complexity. Classification outputs included discrete land cover maps and per-class probability layers, generated using block-wise prediction across the study area.

Derived metrics

Urban change was quantified at the hexagon level using the:

- Change rate represents the proportion of pixels within each hexagon that changed class between the two epochs. This metric captures overall land cover dynamics regardless of transition type [14].
- Delta impervious measures the difference in impervious surface proportion between 2025 and 2017 [15]. Positive values indicate growth in built-up surfaces, while negative values indicate a reduction.
- Urban balance quantifies the net directional change between green-to-impervious and impervious-to-green transitions within each hexagon [16]. Positive values indicate dominant sealing processes, whereas negative values indicate dominant greening processes.
- Green to impervious density was calculated to express the intensity of land cover transitions per unit area. This metric accounts for the spatial concentration of changed pixels within each hexagon and enables comparison of change intensity independently of proportional values.

Spatial agreement between change metrics was assessed using the Jaccard index, calculated as the ratio between the intersection and union of hexagons classified as highly changed.

RESULTS

Land cover accuracy

To evaluate temporal robustness, a reference Random Forest model trained exclusively on 2017 stable samples was applied to 2025 data without retraining. While the model achieved high internal validation performance in 2017 (ACC = 0.95; ROC AUC = 0.98), transfer performance to 2025 decreased substantially (ACC = 0.75; ROC AUC = 0.85; PR AUC = 0.57). The marked reduction in performance indicates the presence of temporal domain shift between the two epochs. Supervised classification models strongly depend on the representativity of training samples, and even images acquired by the same sensor may exhibit shifts in spectral distributions due to differences in acquisition conditions, seasonal variability, or structural land cover changes [7]. Although radiometric normalization was applied, differences in surface structure, urban densification, and spectral heterogeneity reduced model generalizability. In contrast, epoch-specific models trained independently for 2025 achieved substantially higher accuracy. Both RF and XGBoost had strong classification performance in 2017, achieving overall accuracies of 94.5% ($\kappa = 0.89$) and 94.4%, respectively. However, classification performance slightly declined in both ML models for 2025 ($\kappa = 0.76$), while ROC AUC stayed high (~0.965). Misclassification was mostly localized near the impervious–green interface in both epochs, but the "other" class did not significatly change. These results demonstrate that direct model transfer across years are introducing additional uncertainty in change detection analyses. Therefore, epoch-specific training was retained as the primary strategy for land cover mapping, while the transfer experiment serves as an indicator of temporal separability and structural transformation within the urban landscape. To mitigate the limitations of training on disparate samples and to prevent error propagation, a detailed manual validation will be conducted in areas exhibiting the most significant transitions from vegetated to impervious surfaces, in order to quantify the actual change.

Land cover model

The resulting LULC maps indicate that the urban system was predominantly vegetated in both years. In 2017, Urban Green Spaces (UGS) covered 37 km², impervious surfaces covered 14 km², and other surfaces covered 0.46 km². By 2025, impervious surfaces increased to 15 km², UGS decreased to 36.7 km², while the "other" class expanded to 0.66 km² (Figure 2). Proportionally, UGS remained dominant (~70–72%), whereas impervious surfaces rose from approximately 27% to 29% of the total mapped area. Impervious surfaces exhibited the largest absolute change (+1 km²), indicating quantifiable urban growth, while UGS were the most stable category (−0.3 km²). To evaluate methodological sensitivity, RF-derived vegetation estimates were compared against vegetation dynamics obtained from NDVI thresholding (NDVI ≥ 0.3). NDVI thresholding identified 36.7 km² of stable vegetation, 2.66 km² of loss, and 4.53 km² of gain. In contrast, the RF model identified 31.96 km² of stable vegetation, 5.74 km² of loss, and 4.82 km² of gain. The higher vegetation loss estimated by the multi-feature classifier reflects its ability to capture structural and textural transitions that are not resolved by single-index thresholding. This discrepancy therefore represents methodological sensitivity rather than conflicting land cover trends.

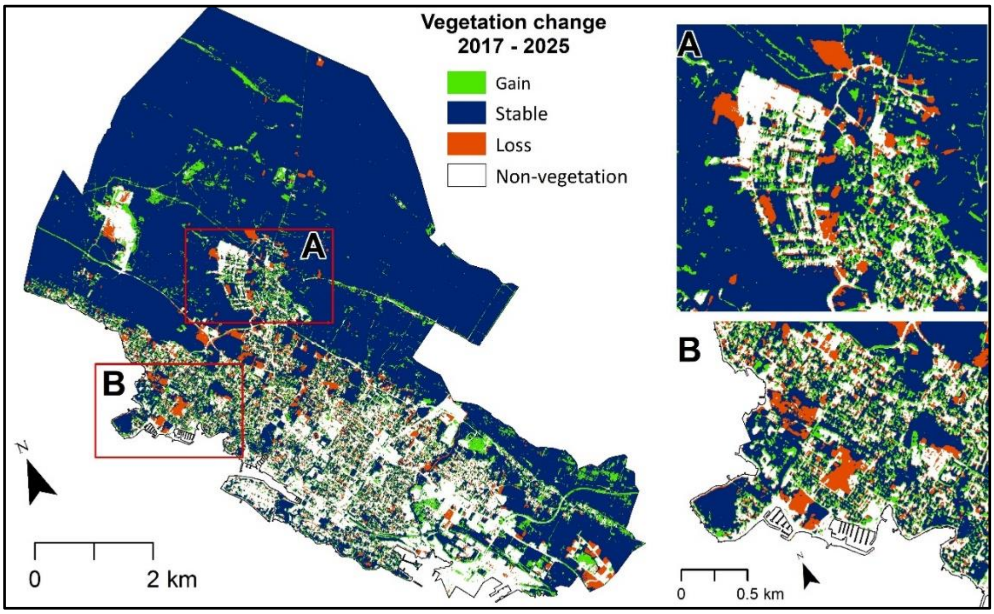

Figure 2. Vegetation change 2017 - 2025

Urban change at the hexagon level

Hexagon analysis pronounced spatial heterogeneity in land cover transitions. The change rate showed that 195 hexagons (51%) are stable, 92 (24%) are moderately changed, and 96 (25%) are highly changed. Maximum change values reaching 0.63 in single polygon.

However, the change in this hexagon were partially associated with transitions between vegetation and the “other” class, showing that not all high-change zones correspond to structural urban transformation. To isolate physical urban growth, the delta impervious metric was analyzed. This metric identified 216 hexagons (56%) as stable, 71 (19%) as moderately increased, and 96 (25%) as highly increased in impervious surface proportion. Thus, 44% of the study area experienced measurable growth in built-up surfaces. The high-change class exhibited a mean impervious increase of 0.109 (median 0.089), with maximum local increases of 0.47, indicating substantial localized urban expansion. To assess whether areas of high overall land cover change correspond to areas of urban expansion, spatial agreement between the change rate and delta impervious metrics was evaluated. While both metrics identified 96 hexagons as highly changed, only 48 hexagons were common to both categories. This corresponds to a Jaccard index of 0.33, indicating moderate spatial agreement. In practical terms, this means that about half of the hexagons exhibiting high overall land cover change were driven by increases in impervious surfaces. The remaining high-change zones were associated with other land cover transitions, such as vegetation dynamics or shifts involving the “other” class. These results underline the importance of separating general land cover variability from structural urban growth when interpreting spatial change patterns.

Table 1. Urban change metrics

Metric	Class	N	%	Mean	Median	Max
Change rate	Stable	195	51	0.1	0.08	0.2
	Moderate	92	24	0.25	0.25	0.31
	High	96	25	0.39	0.37	0.63
Delta impervious	Stable	216	56	−0.04	−0.02	0.01
	Moderate	71	19	0.02	0.02	0.04
	High	96	25	0.11	0.09	0.47
Urban balance	Stable	191	50	0	0	0.04
	Negative	96	25	−0.08	−0.06	−0.56
	Positive	96	25	0.11	0.09	0.47

The urban balance was used to assess the net direction of change, defined as the difference among green to impervious and impervious to green transitions per hexagon. A total of 191 hexagons (50%) were classified as stable, while 96 (25%) negative balance (dominant impervious to green transitions) and 96 (25%) positive balance (dominant green to impervious transitions) (Figure 3). Although the number of positive and negative hexagons was identical, their magnitudes differed. The positive class showed a higher mean intensity compared to the negative class, with maximum values reaching 0.47 and −0.56, respectively (Table 1). Together, these metrics indicate that, despite localized greening processes, the intensity of green-to-impervious transitions exceeded the reverse process.

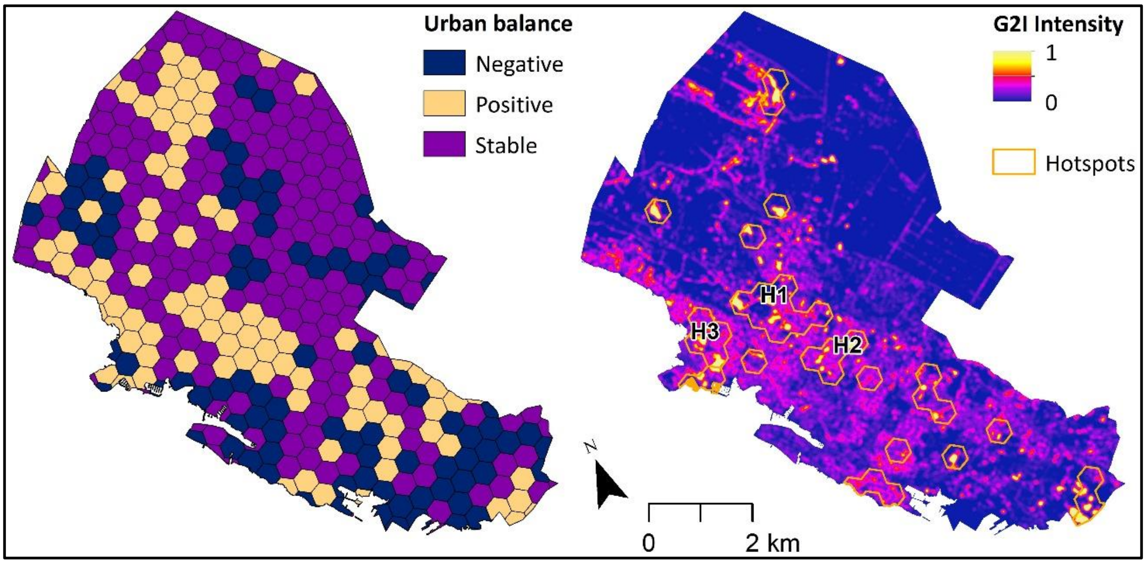

Figure 3. Urban balance (left) and Green to Imprevioss change intensity hotspots (right)

The kernel density map of high delta impervious hexagons (G2Intensity) highlights clear spatial clustering of urban growth rather than a uniform distribution across the study area (Figure 3). High-density zones are predominantly concentrated in central and transitional urban sectors, with secondary clusters emerging along peripheral development corridors. In contrast, northern and outer areas exhibit substantially lower change intensity, indicating spatially uneven urban dynamics. The identified hotspots represent areas where high-intensity impervious surface expansion is spatially aggregated, suggesting coherent development processes rather than isolated local transitions. Based on the density surface, three compact and spatially contiguous hotspot polygons were delineated. These zones correspond to the most concentrated areas of impervious surface growth and reflect structurally coherent urban expansion patterns (Figure 4).

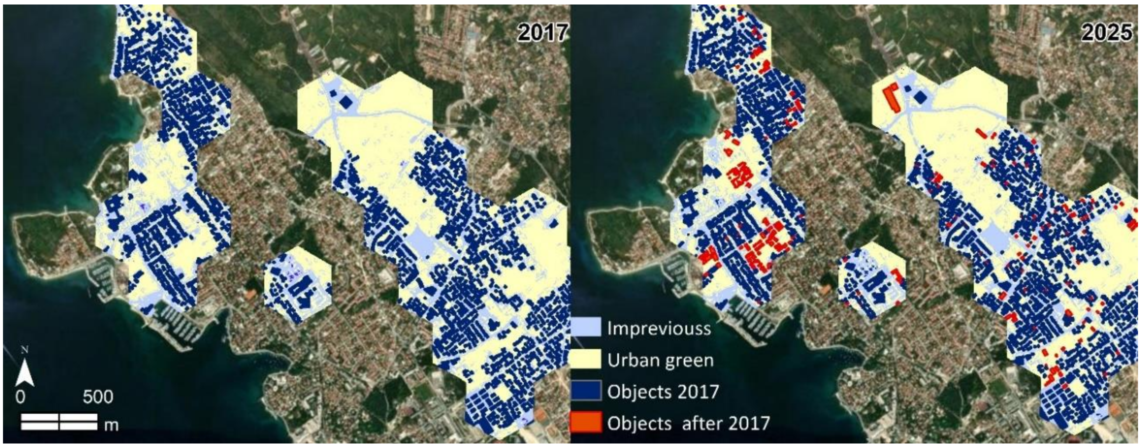

Figure 4. Hotspots of urban change

CONCLUSION

The results confirm that multi-temporal urban mapping is strongly affected by temporal domain shift, as models trained on one epoch do not necessarily generalize reliably to subsequent acquisitions. Even after radiometric normalization, structural transformation and evolving spectral heterogeneity reduced model transferability, emphasizing the importance of epoch-specific training for robust change detection. Spatial aggregation at the hexagon level revealed concentrated zones of impervious surface expansion, indicating spatially uneven urban transformation rather than uniform growth. Comparison between multi-feature classification and NDVI thresholding further demonstrated methodological sensitivity in vegetation change estimation, highlighting the added value of integrating spectral, index-based, and textural features for detecting structural transitions. Future research should focus on integrating multi-annual or sub-annual satellite time series to better capture temporal trajectories of urban change and distinguish gradual from abrupt transformations. Expanding thematic detail beyond aggregated classes and exploring adaptive or transfer-learning approaches may further improve model generalization across temporal domains. In addition, coupling high-resolution remote sensing with urban planning indicators and hydrological parameters could provide a stronger basis for assessing urban resilience and supporting evidence-based spatial management in rapidly transforming Mediterranean cities.

REFERENCES

[1] United Nations, Department of Economic and Social Affairs, Population Division (2018). World Urbanization Prospects: The 2018 Revision. New York: United Nations.

[2] G. Zaro, A. Blaće, J. Baraka Perica, M. Čelhar, F. Jurković Pešić, and K. Gusar, 'Fleeting fields of Zadar (Croatia): characterizing millennial-scale urban landcover change, green space, and resilience into the twenty first century', *Front. Ecol. Evol.*, vol. 11, Sep. 2023, doi: 10.3389/fevo.2023.1221730.

[3] N. Kabisch, H. Korn, J. Stadler, and A. Bonn, 'Nature-Based Solutions to Climate Change Adaptation in Urban Areas—Linkages Between Science, Policy and Practice', in *Nature-Based Solutions to Climate Change Adaptation in Urban Areas: Linkages between Science, Policy and Practice*, N. Kabisch, H. Korn, J. Stadler, and A. Bonn, Eds, Cham: Springer International Publishing, 2017, pp. 1–11. doi: 10.1007/978-3-319-56091-5_1.

[4] R. Milošević, S. Šiljeg, and F. Domazetović, *GIS Multicriteria Decision Analysis in Selecting the Optimal Location for Urban Green Space: A Case Study of Zadar City*. 2023, p. 243. doi: 10.5220/0012031400003473.

[5] C. Kabeja, R. Li, D. E. R. Rwatangabo, and J. Duan, 'Monitoring Land Use/Cover Changes by Using Multi-Temporal Remote Sensing for Urban Hydrological Assessment: A Case Study in Beijing, China', *Remote Sens.*, vol. 14, no. 17, Aug. 2022, doi: 10.3390/rs14174273.

[6] B. E. Lefulebe, A. V. der Walt, and S. Xulu, 'Fine-Scale Classification of Urban Land Use and Land Cover with PlanetScope Imagery and Machine Learning Strategies in the City of Cape Town, South Africa', *Sustainability*, vol. 14, no. 15, Jul. 2022, doi: 10.3390/su14159139.

[7] D. Tuia, C. Persello, and L. Bruzzone, 'Domain Adaptation for the Classification of Remote Sensing Data: An Overview of Recent Advances', *IEEE Geosci. Remote Sens. Mag.*, vol. 4, no. 2, pp. 41–57, Jun. 2016, doi: 10.1109/MGRS.2016.2548504.

[8] L. Panđa, *Imperviousness Density Mapping Based on GIS-MCDA and High-Resolution Worldview-2 Imagery*. 2023, p. 229. doi: 10.5220/0011988200003473.

[9] 'DHMZ - Državni hidrometeorološki zavod'. Accessed: Feb. 16, 2026. [Online]. Available: https://meteo.hr/objave_najave_natjecaji.php?section=onn&param=objave&el=priopcenja&daj=pr12092017

[10] D. Magaš, 'Neke promeje u gradskim naseljima zadarske regije u razdoblju 1857. - 1971. godine', *Rad. Zavoda Za Povij. Znan. HAZU U Zadru*, no. 33, pp. 239–258, Oct. 1991.

[11] V. Graovac, 'Populacijski razvoj Zadra', *Geoadria*, vol. 9, no. 1, pp. 51–72, Jun. 2004, doi: 10.15291/geoadria.129.

[12] Državni zavod za statitstkiku 'Popis 2021.', dzs.gov.hr. Accessed: Feb. 16, 2026. [Online]. Available: https://dzs.gov.hr/u-fokusu/popis-2021/88

[13] S. Hallegatte, C. Green, R. J. Nicholls, and J. Corfee-Morlot, 'Future flood losses in major coastal cities', *Nat. Clim. Change*, vol. 3, no. 9, pp. 802–806, Sep. 2013, doi: 10.1038/nclimate1979.

[14] S. Z. Aldwaik and R. G. Pontius, 'Intensity analysis to unify measurements of size and stationarity of land changes by interval, category, and transition', *Landsc. Urban Plan.*, vol. 106, no. 1, pp. 103–114, May 2012, doi: 10.1016/j.landurbplan.2012.02.010.

[15] W. Kuang, Y. Hou, Y. Dou, D. Lu, and S. Yang, 'Mapping Global Urban Impervious Surface and Green Space Fractions Using Google Earth Engine', *Remote Sens.*, vol. 13, no. 20, Oct. 2021, doi: 10.3390/rs13204187.

[16] G. Zulian, F. Marando, L. Mentaschi, C. Alzetta, B. Wilk, and J. Maes, 'Green balance in urban areas as an indicator for policy support: a multi-level application', *One Ecosyst.*, vol. 7, p. e72685, Mar. 2022, doi: 10.3897/oneeco.7.e72685.